Superalloys 2012: 12th International Symposium on Superalloys
Edited by: Eric S. Huron, Roger C. Reed, Mark C. Hardy, Michael J. Mills, Rick E. Montero, Pedro D. Portella, Jack Telesman
TMS (The Minerals, Metals & Materials Society), 2012

DEVELOPMENT OF AN OXIDATION-RESISTANT HIGH-STRENGTH SIXTH-GENERATION SINGLE-CRYSTAL SUPERALLOY TMS-238

Kyoko Kawagishi[1], An-Chou Yeh[2,3], Tadaharu Yokokawa[1], Toshiharu Kobayashi[2], Yutaka Koizumi[2] and Hiroshi Harada[2]
[1]High Temperature Materials Unit, Environment and Energy Materials Division, National Institute for Materials Science, 1-2-1 Sengen, Tsukuba, Ibaraki, 305-0047, Japan
[2] Environment and Energy Materials Division, National Institute for Materials Science, 1-2-1 Sengen, Tsukuba, Ibaraki, 305-0047, Japan
[3] Current affiliation: Materials Science and Engineering Department, National Tsing Hua University, Taiwan (R.O.C.)

Keywords: Single Crystal superalloy; 6th generation, Creep property, Environmental property

Abstract

For jet engines to meet the ever-increasing demands of ecological compatibility, the compositions of Ni-base single-crystal superalloys have continuously evolved to cope with the increase in turbine entry temperature (TET) owing to the design that improve the thermodynamic efficiency of gas turbine engines. Over the past decade, the addition of Ru has been one of the main subjects of focus to enhance the temperature capability and contribute to the development of new generations of single-crystal superalloys. This paper reposts one of the latest Ru-bearing 6th generation superalloys developed by the National Institute for Materials Science (NIMS), TMS-238. TMS-238 is a promising candidate alloy for future turbine blade applications because it exhibits excellent and well-balanced mechanical and environmental properties.

Introduction

Ni-base single-crystal superalloys have excellent high-temperature properties, and advances in the temperature capability of these materials have led to an increase in the efficiency of jet engines and gas turbines. 4th generation Ni-base superalloys contain 2–3 wt% Ru, which hinders the precipitation of topologically close packed (TCP) phases [1] and improves the high-temperature microstructure stability [2–4]. 4th generation superalloys have achieved temperature capabilities 30°C higher on average than those of the previous generation superalloys in terms of high-temperature creep strength. 5th generation superalloys have been invented by the optimization of alloying compositions, and the content of Ru has increased to 5–6wt%; the lattice misfit between the γ and the γ′ phases has been controlled to balance the interfacial strengthening and coherency, and the dislocation network at the interface of the γ and the γ′ phases has become finer than that of 4th generation superalloys in order to inhibit dislocation migration under stress. Thus, the high-temperature creep resistance of 5th generation superalloys is better than that of 4th generation superalloys [5].

However, these 4th and 5th generations of superalloys are likely to have lower resistance against oxidation than the previous generations owing to the higher content of refractory elements such as Mo, Re and Ru [6, 7]. These refractory-based oxide species have relatively higher vapor pressures and can disrupt the continuity of protective Al_2O_3 formed on the surface during thermal exposure. To make 4th and 5th generation superalloys commercially viable, an improvement in oxidation resistance is imperative. In this study, a 6th generation superalloy, TMS-238, which exhibits both high-temperature creep strength and improved oxidation resistance, has been developed. The alloy design procedure involves utilizing the composition of TMS-196 [8] as a base to optimize the alloy chemistry so as to improve the oxidation resistance and creep strength. High-temperature properties such as creep, oxidation and hot-corrosion resistances have been evaluated for this new superalloy; the experimental results have been compared with those of a 2nd generation superalloy CMSX-4 and a 4th generation superalloy MX-4/PWA1497.

Experimental Procedure

TMS-138A, TMS-196 and TMS-238 were designed by using the Alloy Design Program [9] developed by NIMS. TMS-138A [10] is a 4th generation superalloy containing 5.8 wt% Re and 3.6 wt% Ru. TMS-196 is a 5th generation superalloy containing higher content of Re and Ru (6.4 wt% Re and 5.0 wt% Ru) to realize better mechanical properties than TMS-138A and to improve the oxidation properties by adding Cr. TMS-238 was designed to have mechanical properties similar to TMS-196 but improved oxidation and hot-corrosion resistances. The Mo and W contents were reduced and the Co and Ta contents were increased. The compositions of alloys used in this study are shown in Table 1. The single-crystal samples used for our experiments were vacuum-induction melted and fabricated using a standard directional solidification casting furnace. Materials were supplied as 10-mm cylindrical bars with orientations within 10 degrees of the [001] orientation. Then samples were solution heat treated and aged with no residual eutectics and no visible TCP phases in the microstructures.

Tensile specimens of 4 mm in diameter and 22 mm in gauge length were machined from the heat-treated samples, and tensile tests were conducted at 400°C and 750°C. Tensile creep-upture tests were also conducted on heat-treated samples; specimens were machined into standard creep specimens and tested along the [001] direction to rupture under the following conditions: 800°C/735 MPa, 900°C/392 MPa, 1000°C/245 MPa and 1100°C/137 MPa.

High-temperature cyclic oxidation tests were conducted at 1100°C in air for 1 h per cycle. Specimens were machined to 9 mm in diameter and 5 mm in thickness, and the surfaces were finished with 600-grade SiC paper polishing followed by cleaning with acetone. The change in weight of each specimen was measured at the end of each cycle. The hot-corrosion property was also investigated. Specimens measuring 9 mm in diameter by 5 mm in thickness were soaked in 75%Na_2SO_4+25%NaCl molten salt at

Table 1. Nominal compositions (wt%, Ni bal.).

Alloy	Co	Cr	Mo	W	Al	Ti	Ta	Hf	Re	Ru
CMSX-4	9.6	6.4	0.6	6.4	5.6	1.0	6.5	0.1	3.0	0.0
MX-4/PWA1497	16.5	2.0	2.0	6.0	5.55	0.0	8.25	0.15	5.95	3.0
TMS-138A	5.8	3.2	2.8	5.6	5.7	0.0	5.6	0.1	5.8	3.6
TMS-196	5.6	4.6	2.4	5.0	5.6	0.0	5.6	0.1	6.4	5.0
TMS-238	6.5	4.6	1.1	4.0	5.9	0.0	7.6	0.1	6.4	5.0

Table 2. 0.2% yield stress and UTS at 400°C and 750°C (MPa).

Alloy	400°C		750°C	
	0.2% yield	UTS	0.2%yield	UTS
CMSX-4	860	950	950	1150
TMS-138A	830	906	868	1241
TMS-196	879	1214	845	1308
TMS-238	925	1373	1041	1348

900°C for 20 h. Metal losses in thickness were calculated from weight losses after this 20-h soak.

Results and Analysis

In this section, the experimental results are presented and analyzed. Table 2 shows the results of tensile tests conducted at 400°C and 750°C. The 0.2% yield stress and UTS of TMS-138A are comparable with those of CMSX-4 at both temperatures; TMS-196 shows some improvement and TMS-238 exhibits the highest yield stress and UTS. Figure 1 shows creep performances of CMSX-4, MX-4/PWA1497, TMS-138A, TMS-196 and TMS-238 with respect to the Larson-Miller Parameter. The creep-rupture lives of TMS-238 are comparable to those of TMS-138A and TMS-196 at 800°C/735 MPa, 900°C/392 MPa, and 1000°C/245 MPa. Interestingly, the creep-rupture life of TMS-238 is significantly greater than that of TMS-138A and TMS-196 at 1100°C/137 MPa, although the content of Mo in TMS-238 is less than that in TMS-138A and TMS-196. All the TMS alloys perform better than CMSX-4, and exhibits a performance similarly to MX-4/PWA1497 at 900°C/392 MPa. The advantage of TMS alloys is much more pronounced at lower temperatures/higher stress and higher temperatures/lower stress conditions. Microstructure observations of crept specimens at 1100°C/137 MPa are shown in Fig. 2. Finest lamellar structure found in TMS-238 attributed to its excellent creep property.

The oxidation property was investigated and is shown in Fig. 3. TMS-196 showed an improvement over TMS-138A and has excellent oxidation resistance compared with other 4^{th} and 5^{th} generation superalloys [11]: however, it shows a large decrease in mass in the cyclic oxidation test because of scale spallation, and the oxidation resistance is still inferior to CMSX-4. CMSX-4 shows a relatively stable profile but a slight decrease in mass is found after 50 cycles. Interestingly, TMS-238 shows a constant and gentle increase in mass change until 500 cycles and above. Cross-section images of oxide scales after 1 h of isothermal oxidation at 1100°C were observed and are shown in Fig. 4. TMS-138A forms a very thick NiO layer at the surface, and spinel layer and thick internal Al_2O_3 dispersion zones are formed beneath the NiO layer. CMSX-4, TMS-196 and TMS-238 show a similar oxide structure consisting of NiO, complex oxides and a protective Al_2O_3 layer. The scale thicknesses of CMSX-4 and TMS-238 are almost equal and thinner than that of TMS-196. Kirkendall voids were found beneath the Al_2O_3 layer in TMS-196 and TMS-238. From these observations, it is clear that TMS-238 has superior oxidation resistance compared with CMSX-4 at 1100°C, although it contains less Cr and more Mo and Ru than CMSX-4. It is possible that the higher Ta and lower W content may be beneficial in improving the oxidation resistance of TMS-238.

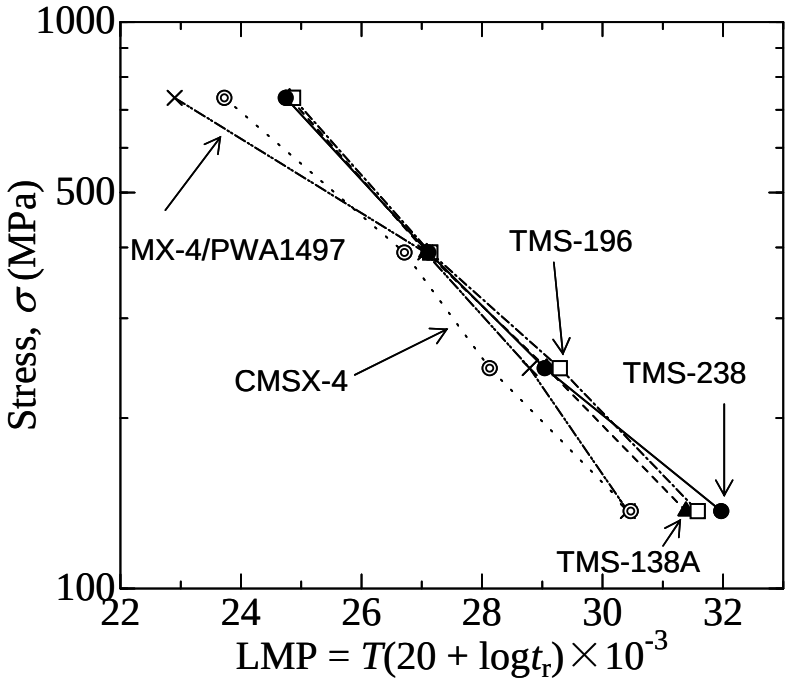

Figure 1. Larson-Miller diagram of creep properties of the investigated alloys.

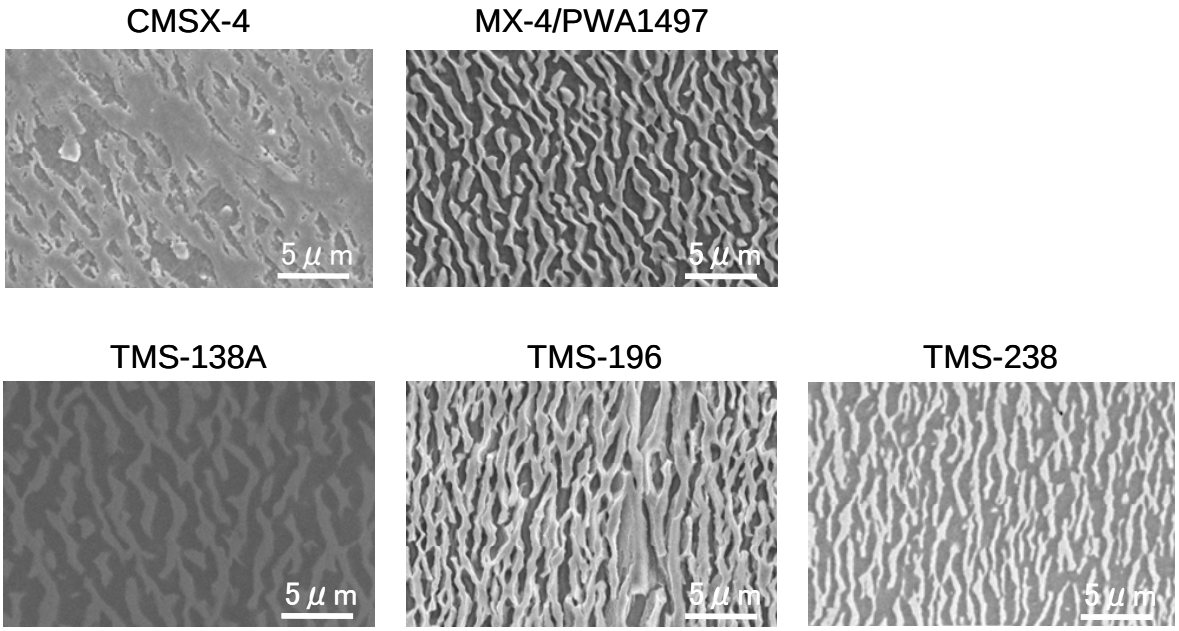

Figure 2. 1100°C /137 MPa crept microstructures of the investigated alloys.

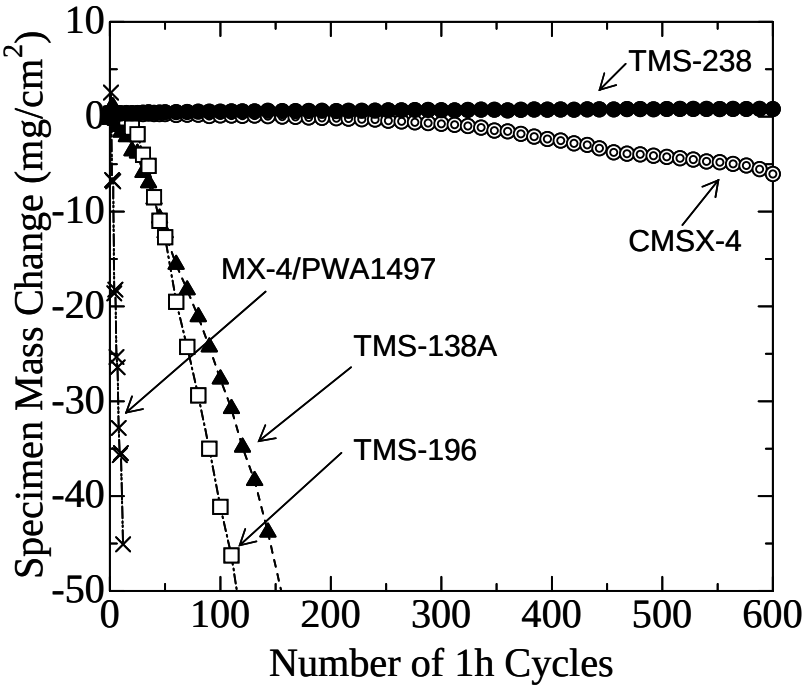

Figure 3. Results of 1100°C cyclic oxidation tests.

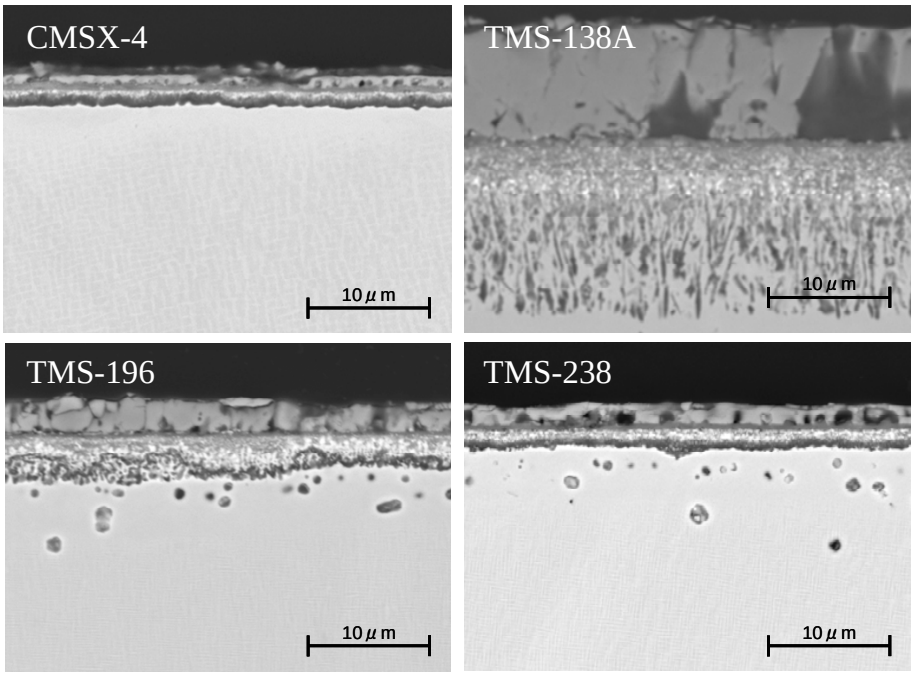

Figure 4. Microstructures after 1 h exposure at 1100°C.

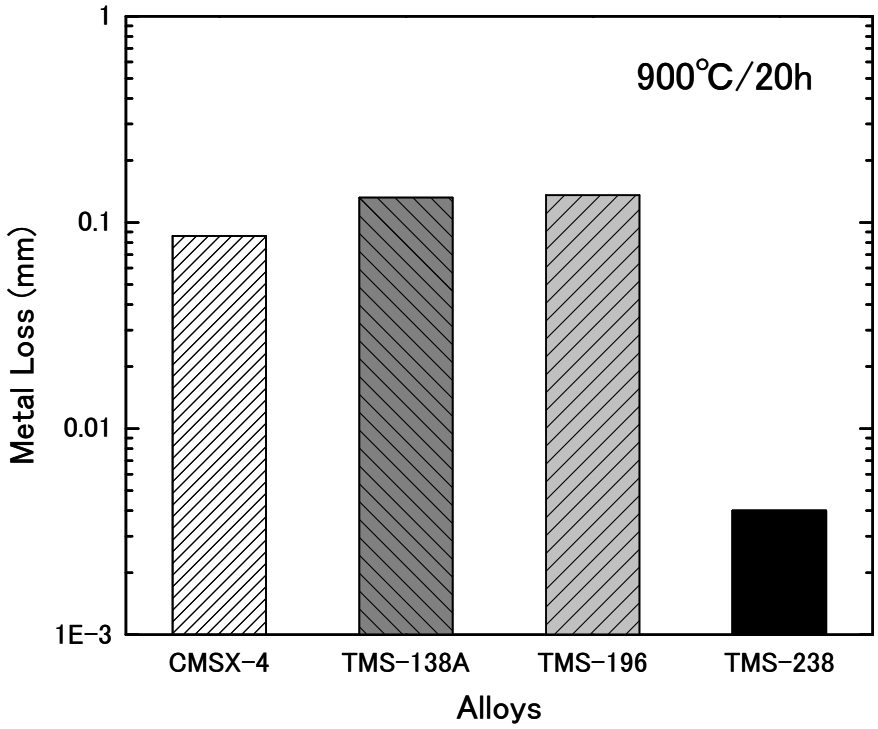

Figure 5. Results of hot−corrosion tests.

Hot-corrosion resistance was evaluated by a crucible test, and Fig. 5 shows the metal losses of CMSX-4, TMS-196 and TMS-238 after 20 h of soaking. TMS-238 had by far the lowest metal loss; hence, this alloy exhibits the best hot-corrosion resistance. It is likely that a lower Mo content and a higher Re content are responsible for this excellent property. Further investigation is required to elucidate the underlying mechanisms.

Figure 6 shows the relationship between creep property and the oxidation resistance. The vertical axis is the oxidation resistance at 1100°C, which was originally defined as including the factors of isothermal mass increase and cyclic mass decrease, and it is expressed as

$$\text{Oxidation Resistance} = \log\left(\frac{1}{w_1} \times \frac{1}{|w_{50} - w_1|}\right) \qquad (1)$$

where w_1 is mass gain after the 1st cycle and $w_{50}-w_1$ is the mass change from the 1st cycle to the 50th cycle in a 1100°C cyclic oxidation test. In this equation, $1/w_1$ is the isothermal oxidation resistance and a $1/|w_{50}-w_1|$ is the cyclic oxidation resistance. A larger value means better durability in both factors, and so the total oxidation resistance is expressed as the increase in the value in the vertical axis in Fig. 6. The horizontal axis indicates the rupture life (h) in the creep test at 1100°C/137 MPa. The open squares, diamonds, triangles and inverted triangles are symbols representing commercial 1st, 2nd, 3rd and 4th generation superalloys. The solid inverted triangle, solid circle and solid double circle stand for NIMS 4th, 5th and 6th generation superalloys. Superalloys were developed focusing on only their mechanical properties up to 4th generation, as shown by the gray arrows in the figure. However, the solid circle and the solid double circle in Fig. 6 show that superalloys with good oxidation resistance and mechanical properties are being developed owing to the recent efforts to improve the oxidation resistance of these alloys. It is evident that TMS-238 has excellent mechanical and environmental properties and that these are in good balance with each other.

Discussion

The composition of alloys influence phase stability, γ/γ′ lattice misfit, microstructural evolutions, and oxides formations, which in turn affect surface stability and mechanical properties. The average γ′ size of a conventional superalloy such as CMSX-4 is 0.5 μm. The lower γ′ solvus temperature and higher Re content in TMS-238 limits the growth of γ′ and slows the rate of diffusion after solution and aging heat treatment. With the addition of Ru, TMS alloys exhibit greater microstructural stability than CMSX-4, although TMS alloys contain a higher amount of refractory elements. This microstructure instability can be attributed to the higher Re and Cr contents, because both elements are very potent

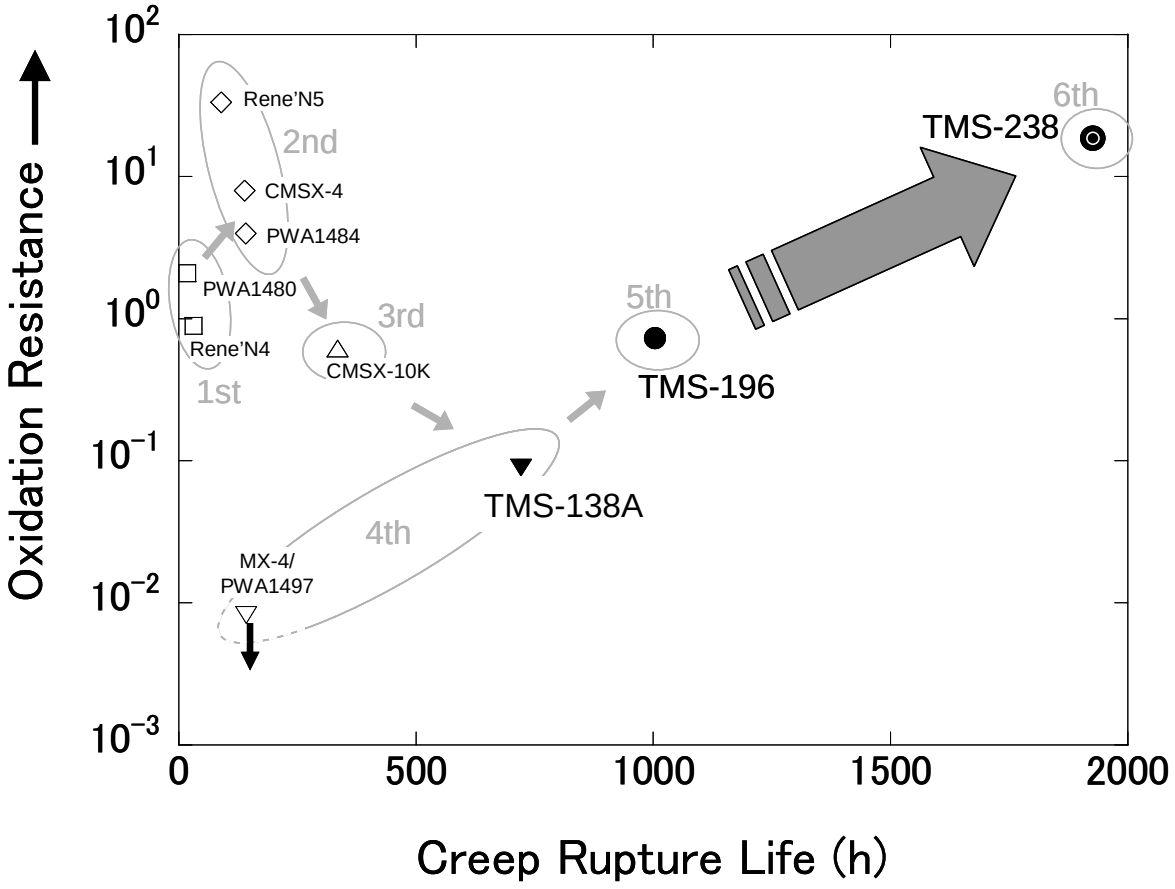

Figure 6. Graph showing comparisons among alloys in terms of a combination of 1100°C/137 MPa creep and 1100°C oxidation resistances.

in forming TCP phases; Re tends to heavily segregate into the dendritic core, in which TCP precipitates can first be observed. However, further reducing the residual Re segregation by added solution heat treatment can reduce the tendency for TCP and δ phase formation in TMS alloys. A previous study [10] suggests that a high Ru content in superalloys may not necessary imply greater microstructural stability, because the overall chemical composition needs to be balanced to prevent precipitations of both TCP and δ phases.

The differences between the creep behaviors of CMSX-4 and TMS alloys demonstrate the important role of γ/γ′ lattice misfit in influencing deformation mechanisms. The γ/γ′ lattice misfit of TMS alloys compared with that of CMSX-4 is more negative owing to the higher amounts of Re and Ru that partition preferentially into the γ phase and expand the lattice parameter of γ. Increasing the γ/γ′ lattice misfit toward the negative not only enhances the rafting kinetics but also refines the dislocation network at the γ/γ′ interface during high-temperature creep. Although the formation of a raft is beneficial against creep in a high-temperature/low-stress condition, the rafted microstructure can be detrimental under intermediate-temperature/intermediate-stress creep condition [10].

It is very interesting to note that TMS-238 exhibits both strong creep and oxidation resistances, and the alloy composition has a higher Ta contents; the Mo content is relatively low to minimize the degradation in oxidation resistance typically observed in this class of superalloys that contain large amount of refractory elements. Furthermore, TMS-238 has been designed to exhibit a slightly smaller lattice misfit between the γ and γ′ phases compared with TMS-196, so as to retain a greater coherency of the microstructure after heat treatment. For TMS-238, the combination of greater microstructure stability and an optimized refractory content result in an alloy exhibiting impressive resistances against creep, hot corrosion and oxidation.

Conclusions

Our recent work at NIMS shows that advanced 5th generation superalloys can be developed having excellent resistance against high-temperature creep, oxidation and corrosion. This paper demonstrates that the TMS-238 superalloy is a promising candidate alloy for turbine blade applications, because this material possesses a balance of the properties desired by gas turbine engine manufacturers to improve engine efficiency. We

believe that our 6th generation single-crystal superalloy TMS-238 has the most excellent and well-balanced mechanical and environmental properties among the existing superalloys.

Acknowledgements

The authors acknowledge the financial support partly provided by Rolls-Royce plc for this research.

References

1. A. Sato, Y. Koizumi, T. Kobayashi, T. Yokokawa, H. Harada and H. Imai, "TTT Diagram for TCP Phases Precipitations of 4th Generation Ni-Base Superalloys", *J Japan Inst Metals*, 68 (2004), pp. 507–510.
2. K. O'Hara, W.S. Walston, E.W. Ross and R. Darolia, U.S. Patent 5,482,789, "Nickel Base Superalloy and Article", 1996.
3. Y. Koizumi, T. Kobayashi, T. Yokokawa, H. Harada, Y. Aoki, M. Arai, S. Masaki and K. Chikugo, "Development of 4th Generation Single Crystal Superalloys", Proceedings (2nd International Symposium on High Temperature Materials, Tsukuba, Japan, 31 May – 2 June 2001), pp. 30–31.
4. J. X. Zhang, T. Murakumo, Y. Koizumi, T. Kobayashi, H. Harada and S. Masaki, "Interfacial Dislocation Networks Strengthening a Fourth-Generation Single-Crystal TMS-138 Superalloy", *Metall. Mater. Trans. A*, 33A (2002), pp. 3741–3746.
5. Y. Koizumi, T. Kobayashi, T. Yokokawa, J. X. Zhang, M. Osawa, H. Harada, Y Aoki and M. Arai, "Development of Next-Generation Ni-Base Single Crystal Superalloys", *Superalloys 2004*, (TMS, 2004), pp. 35–43.
6. S. Walston, A. Cetel, R. MacKay, K. O'Hara, D. Duhl and R. Dreshfield, "Joint Development of a Fourth Generation Single Crystal Superalloy", *Superalloys 2004*, (TMS, 2004), pp. 15–24.
7. K. Kawagishi, A. Sato, T. Kobayashi and H. Harada, "Effect of Alloying Elements on the Oxidation Resistance of 4th Generation Ni-base Single-crystal Superalloys", *J. Japan Inst. Metals*, 69 (2005), pp. 249–252.
8. A. Sato, H. Harada, A. C. Yeh, K. Kawagishi, T. Kobayashi, Y. Koizumi, T. Yokokawa and J. X. Zhang, "A 5th Generation SC Superalloy with Balanced High Temperature Properties and Processability", *Superalloys 2008*, (TMS, 2008), pp.131–138.
9. H. Harada, K. Ohno, T. Yamagata, T. Yokokawa and M. Yamazaki, "Phase Calculation and Its Use in Alloy Design Program for Nickel-Base Superalloys", *Superalloys1988*. (TMS, 1988), pp. 733–742.
10. A. C. Yeh, A. Sato, T. Kobayashi and H. Harada, "On the Creep and Phase Stability of Advanced Ni-base Single Crystal Superalloys", Materials Science and Engineering A, 490 (2008), pp. 445–451.
11. K. Kawagishi, A. Sato, H. Harada, A. C. Yeh, Y. Koizumi, and T. Kobayashi, "Oxidation Resistant Ru Containing Ni Base Single Crystal Superalloys", *Materials Science and Technology*, 25 (2009), pp. 271–275.